

Supplemental Materials

Molecular Biology of the Cell

Raghunathan *et al.*

1 **Supplementary result**

2 **Relation between birth length, length added and length removed during division in**
3 **damage-induced filaments**

4 In general, for an adder system (Si et al., 2019; Wallden et al., 2016; Campos et al., 2014),
5 a very specific relation must hold between the length growth law and the division time's
6 dependence on birth length. If one knows how the length of a cell grows with time, then
7 one can derive this relation. Here, we do this for the particular case where cell lengths
8 grow exponentially with a fixed rate.

9 Let $l(t)$ be the length of a cell at time t , and let $t_{\text{div}}(l_{\text{birth}})$ be the time of next division of a
10 cell that has length l_{birth} when it is created. Here, we assume that t_{div} depends *only* on the
11 birth length of a cell (or rather that all other parameters that may affect t_{div} , such as
12 medium composition, are kept fixed). Then, for an adder system it must be that

13 $l(t_{\text{div}}(l_{\text{birth}})) - l_{\text{birth}} = \text{constant}. \quad (1)$

14 In fact, this constant must be equal to the length of the wild type cell, l_{WT} , so that when
15 the birth length is l_{WT} , the length added before the cell divides is exactly l_{WT} .

16 If cell lengths grow exponentially in time at a fixed rate γ , i.e.,

17 $l(t_2) = l(t_1) \exp(\gamma (t_2 - t_1)), \quad (2)$

18 then combining equations (1) and (2) gives a relation that must be satisfied for an adder
19 with exponentially growing cells.

20 $t_{\text{div}}(l_{\text{birth}}) = \ln(1 + l_{\text{WT}}/l_{\text{birth}}) / \gamma. \quad (3)$

21 **Matlab code for producing the plots in Figure S2**

```
22 % matrix d(:,4) is read from each xlsx file  
23 % d(:,1) = time (min)  
24 % d(:,2) = length (um)  
25 % d(:,3) = length of one of the two cells created upon division (only on rows right after  
26 % where division indicator=1)  
27 % (other cell length can be computed by subtracting this from previous length in  
28 % column 2; note - shorter of the two is by definition the daughter cell, the longer is the  
29 % mother cell)  
30 % d(:,4) = division indicator (0 or 1)  
31  
32 clear all;  
33 f=dir('M*'); % change to 'F*' for ceph cells, no change for MMC cells but make sure xlsx
```

```

34 %files for wild-type cells are not in the same folder
35 n=1;
36 j=1;
37
38 for fi=1:length(f)
39
40 clear d;d=xlsread(f(fi).name);
41
42 tdivnum=find(d(:,4)==1);
43 birthtime=tdivnum(1)+1;
44 for i=2:length(tdivnum) % start looking at data from first division onwards
45 if (tdivnum(i)>birthtime) % no growth curve if divisions at successive time points
46 % calc growth rate from fit to exponential
47 x=d(birthtime:tdivnum(i),1);
48 y=log(d(birthtime:tdivnum(i),2)); SStotal = (length(y)-1) * var(y);
49 rsq(n) = 1 - SSresid/SStotal;
50 numdat(n)=length(x);
51 n=n+1;
52 end
53
54 % calc birth length and div time and length added/removed
55 q(j,1)=d(birthtime-1,2)-d(birthtime,3);
56 q(j,2)=d(tdivnum(i),1)-d(birthtime-1,1);
57 q(j,3)=d(tdivnum(i),2)-d(birthtime-1,2)+d(birthtime,3);
58 q(j,4)=min(d(tdivnum(i)+1,3),d(tdivnum(i),2)-d(tdivnum(i)+1,3));
59 q(j,5)=max(d(tdivnum(i)+1,3),d(tdivnum(i),2)-d(tdivnum(i)+1,3));
60 j=j+1;
61
62 % update birthtime
63 birthtime=tdivnum(i)+1;
64 end
65
66 % now n-1=number of growth curves=length(p), p(:,1)=fitted slope of log growth curve,
67 %p(:,2)=fitted intercept of log growth curve
68 % rsq(:)=R-squared of the fit, numdat(:)=how many data points where in the
69 %corresponding growth curve
70 % and j-1=length(q)=total number of divisions (can be more than number of growth
71 %curves because sometimes a division happens immediately after another
72 % q(:,1)=length at birth, q(:,2)=division time
73 % q(:,3)=length added, q(:,4)=length removed=daughter length just after division,
74 %q(:,5)=mother cell length just after division
75 % q(:,1:3) calculations correct for the fact that there is time delay (typically 2min)
76 %between data points during which time cells lengthen
77 % the formula to get q(:,3) above gives negative values for a few cases in MMC cells -

```

```

78 %this is because sometimes the filament divides in two places simultaneously producing
79 %two daughter cells
80 end
81 figure;
82 fplot(@(x) x,[min(q(:,4)) max(q(:,4))],'r','LineWidth',2);
83 hold on;plot(q(:,5),q(:,4),'k.','MarkerSize',13);
84 xlabel('Mother cell length (\mum)');ylabel('Daughter cell length (\mum)');
85 title('WT cells');
86
87 figure(2);
88 subplot(2,3,1); fplot(@(x) median(p(:,1)),[0 length(p)],'r','LineWidth',2);
89 hold on;scatter([1:length(p)],p(:,1),numdat,1-[rsq' rsq' rsq'],'filled');
90 set(gca,'YLim',[0 0.06]);
91 ylabel('Fitted growth rates (1/min)');xlabel('Cell index');title('WT cells');
92
93 figure;
94 plot(q(:,2),q(:,3),'ro','LineWidth',1);hold on;plot(q(:,2),q(:,4),'b.','MarkerSize',13);
95 set(gca,'YLim',[0 max(max(q(:,3)),max(q(:,4)))]); % making the lower limit of the Y-axis
96 zero hides the divisions where length added comes out to be negative (see above)
97 %legend('Length added','Length removed');
98 xlabel('Division time (min)');ylabel({'Length added (red) and';'removed (blue) in
99 \mum'});title('WT cells');
100
101 figure(2);
102 subplot(2,3,4);plot(q(:,1),q(:,3),'ro','LineWidth',1);hold
103 on;plot(q(:,1),q(:,4),'b.','MarkerSize',13);
104 set(gca,'YLim',[0 max(max(q(:,3)),max(q(:,4)))]);
105 %legend('Length added','Length removed');
106 xlabel('Birth length (\mum)');ylabel({'Length added (red) and';'removed (blue) in
107 \mum'});title('WT cells');
108
109 figure;
110 fplot(@(x) log(1+median(q(:,4))./x)/median(p(:,1)),[0 max(q(:,1))],'r','LineWidth',2);hold
111 on;
112 plot(q(:,1),q(:,2),'k.','MarkerSize',13);
113 set(gca,'YLim',[0 max(q(:,2))]);
114 xlabel('Birth length (\mum)');ylabel('Division time (min)');title('WT cells');
115

```

116 **Supplementary figure legends**

117 **Figure S1: Asymmetric cell division in DNA-damage induced filaments** A. Cell length of
118 L_D and short daughter S_D generated from a DNA damage-induced filament during recovery
119 in M9-Cas. Each grey dot represents a single division event. The red line plots the
120 expected values if all cells were dividing at their mid-point ($n = 402$). B. Distribution of S_D
121 cell lengths for MMC or cephalixin treated filaments. Wild type cell length distribution
122 (asynchronous) is also plotted ($n = 1110$ (wild type), 531 (MMC), 201 (cephalexin)). C. As
123 (A) for cephalixin-treated filaments. ($n = 201$) D. Distribution of relative position of
124 division for filament lengths between 12-40 μm after 30, 60 or 90 min of MMC induction.
125 ($n = 142$ (30 min), 518 (60 min), 95 (90 min)) E-F. Location of division as a function of cell
126 length during recovery from 30 or 90 min DNA damage treatment respectively. ($n = 144$
127 (30 min), 120 (90 min)). G. As (A) for 90 min of damage treatment ($n = 149$). H-I. As (E) for
128 recovery in M9-Cas and cephalixin treatment respectively. ($n = 402$ and 201) J.
129 Percentage of cells carrying ≤ 2 or > 2 RecA-mCherry foci for L_D and S_D during recovery
130 time-lapse from MMC is plotted. ($n = 200$). K. As a control for (J) percentage of cells
131 carrying ≤ 2 or > 2 RecA-mCherry foci binned by cell length after treatment with cephalixin
132 for 1 hr is plotted. Cephalixin causes cellular elongation without DNA damage. An
133 increase in length does not result in an increase in foci number, indicating that L_D retain
134 damage foci, while S_D inherit damage-free chromosomes ($n = 100$) L. CFU/ ml is plotted
135 for no damage control (grey), and DNA damage recovery after 30 (dashed and dotted), 60
136 (dashed) or 90 (dotted) min of damage exposure. OD_{600} of the culture is normalized to
137 0.05 while plating for each time point ($n = 3$ independent repeats, mean and std. dev is
138 shown). M. Cell length distribution during DNA damage recovery time-course for 30 min,
139 60 min and 90 min durations of damage treatment respectively. Individual dots represent
140 length of a single cell. Black line represents median ($n = 30$ min (1688, 1540, 1049, 969,
141 875, 974, 979, 907, 603, 660, 1107, 1079, 1578, 1265), 60 min (1110, 1403, 778, 742, 914,
142 924, 1348, 1056, 1539, 1487, 930, 969, 1398, 1064), 90 min (866, 936, 386, 615, 289, 467,
143 571, 422, 790, 666, 514, 545, 1007, 551)).

144 **Figure S2: Division dynamics of damage-induced filaments.** A-B. Length vs time curves of
145 the cells are fitted to an exponential function, and the resulting fitted growth rates are
146 plotted as dots. The colour of the dot represents the R^2 value of the fit (black=1; white=0;
147 closer to 1 is a better fit). The size of the dot represents the number of time points in each
148 length vs time curve (the more points, the more reliable the fit). The red line marks the
149 median fitted growth rate. (n = 211 and 492, for MMC-treated and wild type cells
150 respectively). X-axis reflects number of divisions. C. Time between divisions as a function
151 of cell length at birth for wild type cells. Red line shows the relation that would be
152 necessary for the system to be an adder (equation (3) in supplementary results), given
153 that cells are growing exponentially with the rates given in Fig. S2A-B (n = 107). D. Oufiti
154 is used to generate segmented profiles of phase contrast images of cells. These are then
155 used to identify potential sites of constriction and detect division events (automated).
156 Phase profile for cephalexin-treated cell before and after division is plotted. Constriction
157 is marked with an * and divisions are identified by Oufiti.

158 **Figure S3: Role of Min system in division positioning** A. (top) FtsZ-GFP localizations across
159 increasing cell length represented as a kymograph (n = 150). (bottom) Number of FtsZ-
160 GFP localizations against cell length for damage-induced filaments (n = 150). B. (left) As
161 an illustrative example, localization of MinD-GFP in a single MMC or cephalexin treated
162 filament is shown. (right) Number of Min localizations as a function of increasing cell
163 length (n = MMC (266), cephalexin (467)). C. Heat map of transcript levels (from RNA-seq)
164 of genes involved in cell division during a damage recovery time-course. As a control,
165 genes induced under the SOS response are also highlighted (bold). Log₂-fold change
166 normalized to control without damage is plotted. D. Number of constrictions per cell
167 during DNA damage recovery for wild type, *slmA* and *sulA* cells and for cells during
168 cephalexin recovery (n = 140 (wild type), 81 (Δ *slmA*), 69 (Δ *sulA*), 47 (cephalexin)). E.
169 Relative position of division plotted as a function of filament length at division for
170 Δ *minCDE* (n = 186). F. Representative time-lapse montage of division in Δ *minCDE* cells
171 during damage recovery. Asterix marks site of division.

172 **Figure S4: Impact of chromosome and terminus segregation on division regulation** A.
173 Representative time-lapse montage of anucleate division in cells during recovery. Grey –
174 phase, red – HupA-mCherry (chromosome); scale bar - 5 μm ; time in min. Fluorescence
175 intensity traces for the cell in montage is provided below. Division sites are marked with
176 '*'. B. Representative time-lapse montage of FtsZ-GFP localization during damage
177 recovery time-lapse. Grey – phase, red – HupA-mCherry (chromosome), green – FtsZ-
178 GFP. C. Position of least intensity of HupA fluorescence (gaps between chromosomes)
179 plotted against the position of the FtsZ-ring at the time of cell division. Positions are
180 relative to cell length (n = 145). D. Segmentation profile of phase image is plotted in black
181 for a single cell. Time-lapse frames before a constriction (a.) and up to one frame before
182 a division (c.) are shown. Cell length (0) indicates the location at which a constriction is
183 identified and $2 \mu\text{m} \pm$ this location is plotted. Along with phase profile, fluorescence
184 profile of chromosome (red) and *terminus* (green) is shown. Single terminus focus
185 splitting into two is highlighted with an asterix. E. Representative time-lapse montage of
186 *terminus* localization during damage recovery time-lapse. White asterisks highlight
187 *terminus* location prior to division. red – HupA-mCherry (chromosome), green –
188 ParBpMT1-GFP, *parSpMT1* (at *ter*). F. CFU/ ml is plotted for no damage control (grey) and
189 DNA damage recover for wild type (dotted) and ΔmatP (dashed) cells. OD_{600} of the culture
190 is normalized to 0.05 while plating for each time point (three independent repeats). G.
191 CFU/ml is plotted without damage for wild type and ΔmatP . No significant difference was
192 observed (unpaired T-test; three independent repeats).

193 **Figure S5: Asymmetric chromosome segregation and cell division in DNA damage-**
194 **induced *Escherichia coli* filaments**

195 Min oscillations dictate division site positioning. Chromosome segregation additionally
196 influences the timing of division during nucleated cell divisions. Short daughter cells of
197 wild type size tend to be devoid of damage and grow and divide as wild type. For details,
198 see main text.

199

200

201 **Table S1: Strains and plasmids used in this study**

Name	Background	Description	Source/ construction	Experiment
JJC5789	MG1655	MG1655 <i>lac::P_{recA}-recA-mCherry (chl)</i>	(Vickridge et al., 2017)	Fig. S1J-K
SJ1737	MG1655	MG1655 low motile <i>hupA-mruby2 (chl)(FRT); P1 parS @ 33.7' (kan); pALA2705 (carb) with gfp-parB</i>	(Youngren et al., 2014)	Source for NAB214
NP127	MG1655	MG1655 <i>zapA-gfp hupA-mCherry (Chl)(FRT)</i>	(Buss et al., 2017)	Fig. 4E
NAB94(SR)	BW25113	BW25113 <i>ΔminCDE (kan)</i>	CGSC stock centre	Source for NAB332
SS6282	MG1655	MG1655 <i>hupA-mCherry(kan)(FRT); P_{sulA}-gfp</i>	(Marceau et al., 2011)	Source for NAB227
NAB95(SR)	MG1655	MG1655 <i>P_{ftsZ}-ftsZ-gfp (chl)</i>	(Jena et al., 2020)	Source for NAB98
RSB156	MG1655	MG1655 <i>ΔslmA (tet)</i>	CGSC stock centre	Source for NAB331
NAB96(SR)	MG1655	MG1655 <i>ΔsulA (kan)</i>	CGSC stock centre	Source for NAB329
NAB98	MG1655	MG1655 <i>hupA-mCherry(kan)(FRT); P_{ftsZ}-ftsZ-gfp (chl)</i>	This study <i>hupA-mCherry was transduced into MG1655. Kanamycin cassette was flipped out using the FRT sites flanking the antibiotic (NAB227). Following this, P_{ftsZ}-ftsZ-gfp (chl) was transduced into this strain. Verified via microscopy</i>	Fig. 4E, G. S3. A and S4. B-C
NAB99(SR)	MG1655	MG1655 <i>ΔmatP (kan)</i>	<i>ΔmatP (kan) from CGSC stock centre in MG1655 background. Verified by PCR</i>	Fig. 4F and S4. F-G
NAB214	MG1655	MG1655 <i>hupA-mCherry(kan)(FRT); P1 parS @ 33.7' (kan); pALA2705 (amp) with gfp-parB</i>	This study <i>P1 parS @ 33.7' (kan) was transduced into MG1655 hupA-mCherry (FRT) (NAB227); pALA2705 (amp) was transformed into this. Verified by microscopy</i>	Fig. 4E and S4. D-E

NAB227	MG1655	MG1655 <i>hupA</i> - <i>mCherry</i>	This study <i>hupA</i> - <i>mCherry</i> (<i>kan</i>) was transduced into MG1655. Kanamycin cassette was flipped out using the FRT sites flanking the antibiotic. Verified by microscopy	Figures pertaining to wild type recovery and chromosome dynamics (HupA)
NAB325	MG1655	MG1655 <i>pNIH299-3</i> <i>P_{lac}</i> <i>egfp-minD minE-mCherry</i> (<i>amp</i>)	This study <i>pNIH299-3</i> was transformed into MG1655. Verified by microscopy	Fig. S3B
NAB329	MG1655	MG1655 Δ <i>sulA</i> (<i>kan</i>); <i>hupA</i> - <i>mCherry</i> ; <i>P_{ftsZ}</i> - <i>ftsZ-gfp</i> (<i>chl</i>)	This study Δ <i>sulA</i> was transduced into NAB98. Strain was verified by PCR	Fig. 3C, S3D and 4F
NAB331	MG1655	MG1655 Δ <i>slmA</i> (<i>tet</i>); <i>hupA</i> - <i>mCherry</i> ; <i>P_{ftsZ}</i> - <i>ftsZ-gfp</i> (<i>chl</i>)	This study Δ <i>slmA</i> was transduced into NAB98. Verified by PCR	Fig. 3B, S3D and 4F
NAB332	MG1655	MG1655 Δ <i>minCD E</i> (<i>kan</i>) <i>hupA</i> - <i>mCherry</i> ; <i>P_{ftsZ}</i> - <i>ftsZ-gfp</i> (<i>chl</i>)	This study Δ <i>minCDE</i> was transduced into NAB98. Verified by PCR	Fig. 3D, S3E-F
NAB341	MG1655	MG1655 <i>hupA</i> - <i>GFP</i> ; <i>pRHmcherryFtsN</i>	This study <i>pRHmcherryFtsN</i> was transformed into NAB98. Verified by microscopy	Fig. 4E
pALA2705	Plasmid in DH5 α	<i>P_{trc90}</i> - <i>gfp-parB</i> (<i>amp</i>)	(Youngren et al., 2014)	Source for NAB214
<i>pRHmCherryFtsN</i>	Plasmid in DH5 α	<i>P_{rha}</i> - <i>mCherry-ftsN</i> (<i>amp</i>)	(Söderström et al., 2018)	Source for NAB341
NIH299-3	Plasmid in DH5 α	<i>P_{lac}</i> <i>egfp-minD minE-mCherry</i> (<i>amp</i>)	Plasmid was made by Genscript. Briefly, <i>EcoR1</i> - <i>mGFPmut3.1</i> - <i>XbaI</i> and <i>BamHI</i> - <i>mCherry</i> - <i>HindIII</i> fragments were synthesized by Genscript. <i>pYLS68</i> (Shih et al., 2002) carrying <i>YFP</i> - <i>minD</i> - <i>minE</i> - <i>CFP</i> was first digested with <i>EcoR1</i> - <i>XbaI</i> to excise <i>YFP</i> and <i>mGFP</i> was ligated into the same. The resultant vector was digested with <i>BamHI</i> - <i>HindIII</i> to excise <i>CFP</i> and <i>mCherry</i> fragment was ligated into the same.	Source for NAB325

203 **Table S2: Oligonucleotides used in this study**

Name	Sequence	Description
SR_Oligo_221	GCGAGGCTCTTCCGAA	<i>sulA</i> upstream forward
SR_Oligo_223	ACCGCTTCAGACAAGCCTC	<i>sulA</i> downstream reverse
SR_Oligo_258	CGGTCATAGCGTGGGTGCCGCC	<i>slmA</i> upstream forward
SR_Oligo_259	ATGGCGGAACATCTGGCGGCGGTTAAGG	<i>slmA</i> downstream reverse
SR_Oligo_264	GTCTTCGGAACATCATCGCGCTGGC	<i>minCDE</i> upstream forward
SR_Oligo_265	TGGGAACAGCCTTAAGGTGTAAAGGGGAGG	<i>minCDE</i> downstream reverse
SR_Oligo_291	CCTGGCATGGGCGTTAAAGC	<i>matP</i> upstream forward
SR_Oligo_292	ACGTTGTA ACTCAGCCGCAGG	<i>matP</i> downstream reverse

204

205 **Supplementary references**

- 206 Buss, J.A., N.T. Peters, J. Xiao, and T.G. Bernhardt. 2017. ZapA and ZapB form an FtsZ-
207 independent structure at midcell. *Mol Microbiol.* 104:652–663.
208 doi:10.1111/mmi.13655.
- 209 Campos, M., I.V. Surovtsev, S. Kato, A. Paintdakhi, B. Beltran, S.E. Ebmeier, and C.
210 Jacobs-Wagner. 2014. A constant size extension drives bacterial cell size
211 homeostasis. *Cell.* 159:1433–1446. doi:10.1016/j.cell.2014.11.022.
- 212 Jena, P., M. Bhattacharya, G. Bhattacharjee, B. Satpati, P. Mukherjee, D. Senapati, and R.
213 Srinivasan. 2020. Bimetallic gold–silver nanoparticles mediate bacterial killing by
214 disrupting the actin cytoskeleton MreB. *Nanoscale.* 12:3731–3749.
215 doi:10.1039/C9NR10700B.
- 216 Marceau, A.H., S. Bahng, S.C. Massoni, N.P. George, S.J. Sandler, K.J. Mariani, and J.L.
217 Keck. 2011. Structure of the SSB-DNA polymerase III interface and its role in DNA
218 replication. *EMBO J.* 30:4236–4247. doi:10.1038/emboj.2011.305.
- 219 Shih, Y.-L., X. Fu, G.F. King, T. Le, and L. Rothfield. 2002. Division site placement in E.coli:
220 mutations that prevent formation of the MinE ring lead to loss of the normal
221 midcell arrest of growth of polar MinD membrane domains. *The EMBO Journal.*
222 21:3347–3357. doi:10.1093/emboj/cdf323.
- 223 Si, F., G. Le Treut, J.T. Sauls, S. Vadia, P.A. Levin, and S. Jun. 2019. Mechanistic Origin of
224 Cell-Size Control and Homeostasis in Bacteria. *Curr. Biol.* 29:1760-1770.e7.
225 doi:10.1016/j.cub.2019.04.062.
- 226 Söderström, B., H. Chan, P.J. Shilling, U. Skoglund, and D.O. Daley. 2018. Spatial
227 separation of FtsZ and FtsN during cell division. *Mol. Microbiol.* 107:387–401.
228 doi:10.1111/mmi.13888.
- 229 Vickridge, E., C. Planchenault, C. Cockram, I.G. Junceda, and O. Espéli. 2017.
230 Management of E. coli sister chromatid cohesion in response to genotoxic stress.
231 *Nature Communications.* 8:14618. doi:10.1038/ncomms14618.
- 232 Wallden, M., D. Fange, E.G. Lundius, Ö. Baltekin, and J. Elf. 2016. The Synchronization of
233 Replication and Division Cycles in Individual E. coli Cells. *Cell.* 166:729–739.
234 doi:10.1016/j.cell.2016.06.052.
- 235 Youngren, B., H.J. Nielsen, S. Jun, and S. Austin. 2014. The multifork Escherichia coli
236 chromosome is a self-duplicating and self-segregating thermodynamic ring
237 polymer. *Genes & Development.* 28:71–84. doi:10.1101/gad.231050.113.

238

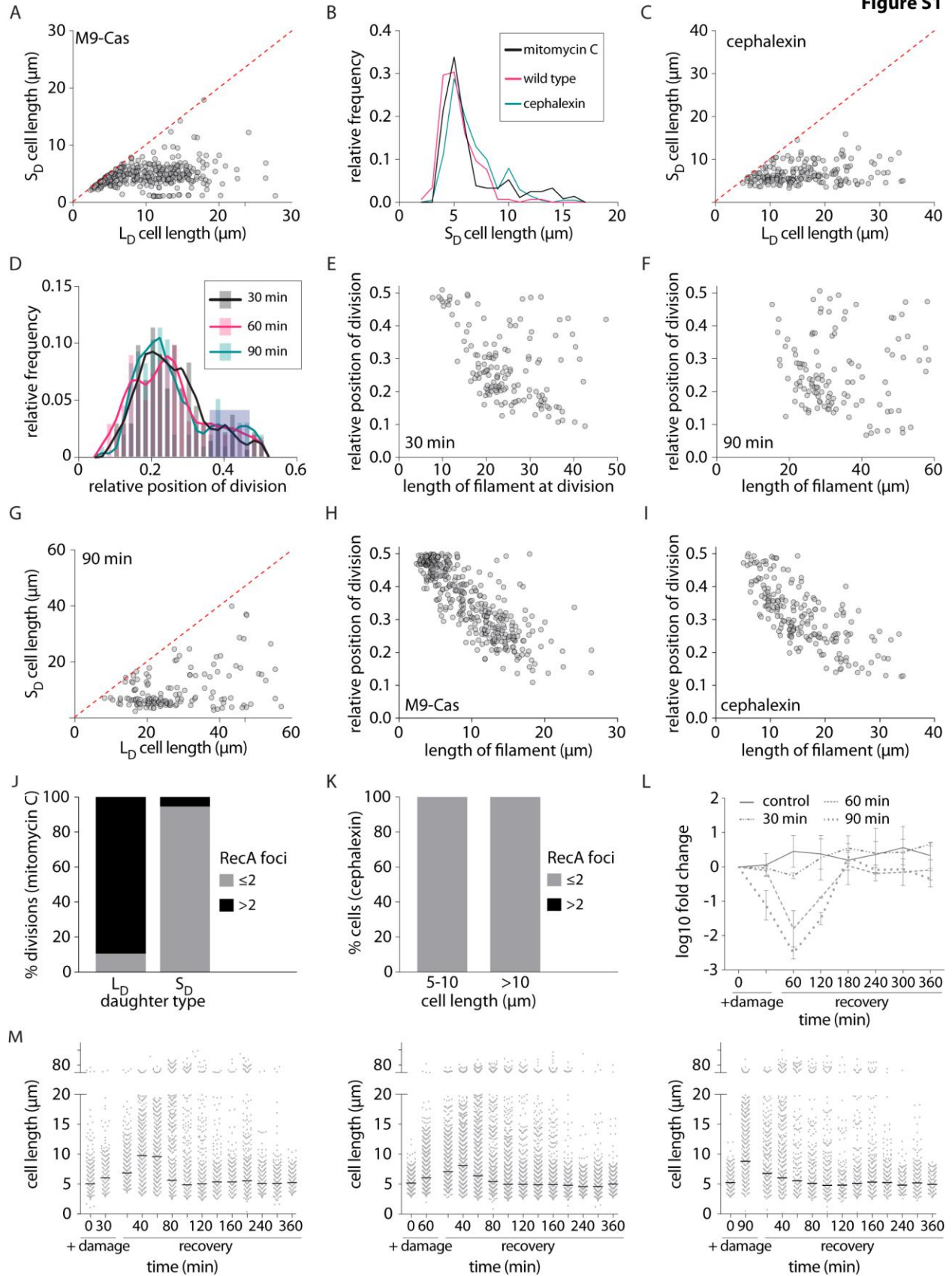
Figure S1

Figure S2

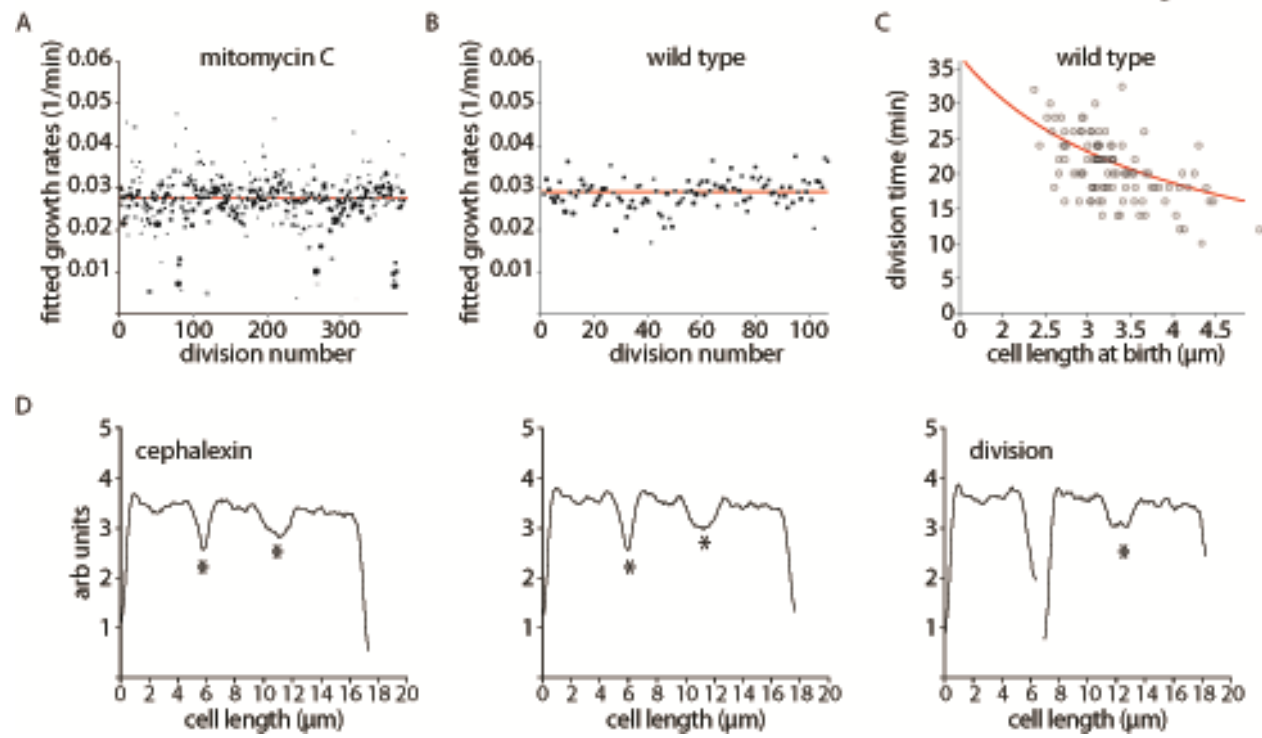


Figure S3

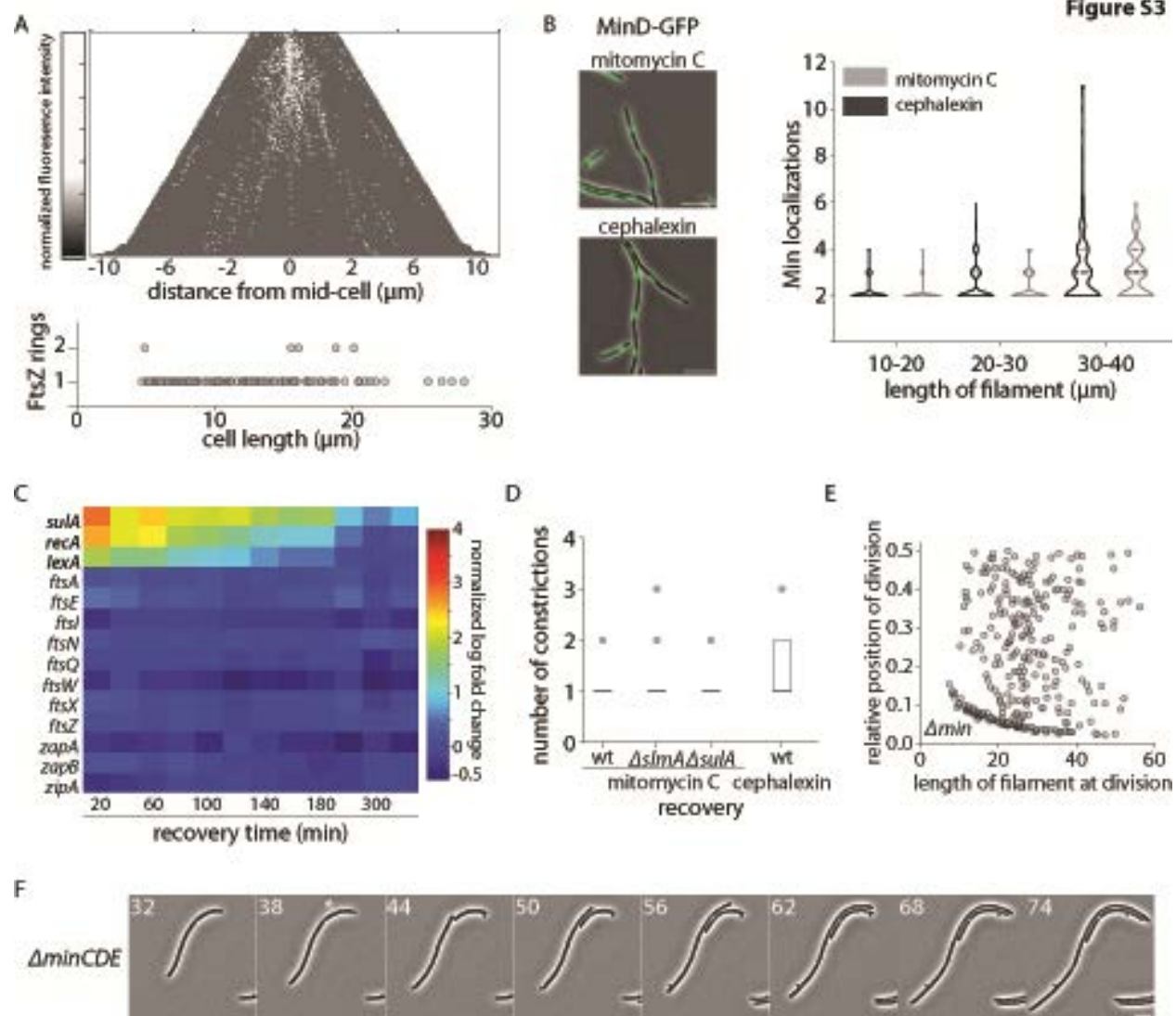


Figure S4

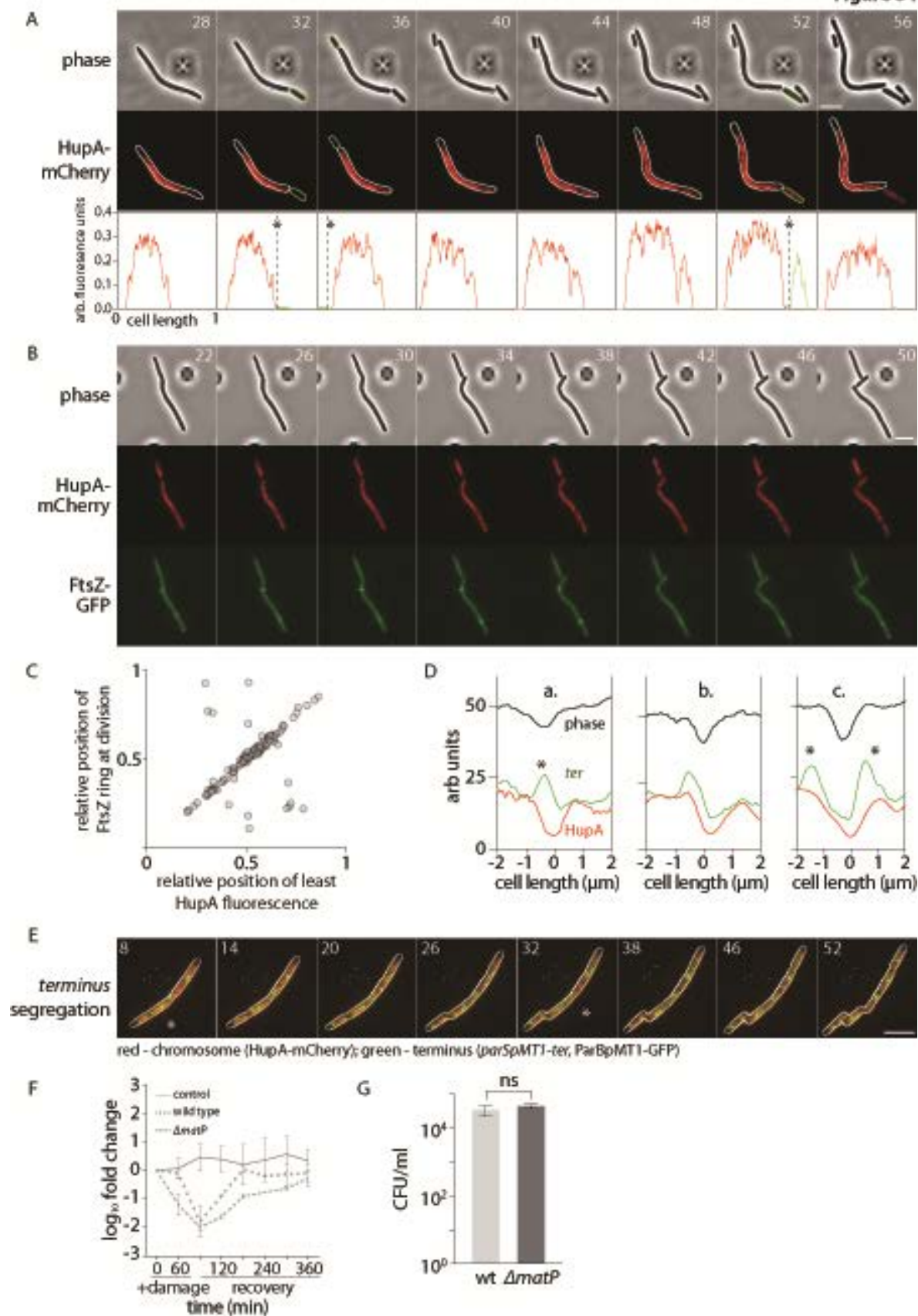


Figure S5

